Measurement of large convex aspheres

J. H. Burge

Steward Observatory Mirror Lab, University of Arizona
Tucson, Arizona 85721

ABSTRACT

Large convex aspheres are notoriously difficult to fabricate because of the tremendous cost and difficulty of making accurate measurements of the optical surfaces. The new 6.5- and 8-m-class telescopes require convex secondary mirrors that are larger, more aspheric, and more accurately figured than those for existing telescopes. Two powerful measurement techniques have been implemented at the Mirror Lab and demonstrated to be accurate and economical. The polished surfaces are interferometrically measured using holographic test plates. This measurement technique uses full-aperture test plates with computer-generated holograms (CGH) fabricated onto spherical reference surfaces. When supported a few millimeters from the secondary and properly illuminated with laser light, an interference pattern is formed that shows the secondary surface errors. The hologram consists of annular rings of metal drawn onto the curved test plate surface using a custom-built writing machine. This test has been implemented for secondaries up to 1.15-m diameter, with 4 nm rms surface measurement accuracy. In addition to this test, a swing arm profilometer was built to measure the rough surface during aspherization and loose abrasive grinding. The machine uses simple motions and high quality components to achieve 50 nm rms measurement accuracy over 1.8-m mirrors.

Keywords: optical testing, interferometry, computer-generated holograms, profilometry.

1. INTRODUCTION

Large ground-based telescope projects are currently underway that require primary mirrors as large as 8.4 meters in diameter and as fast as $f/1$. Since the primary mirrors are concave, they can be interferometrically measured from center of curvature using null correctors. The secondary mirrors for these giant telescopes are often convex, steeply aspheric, and large (up to 1.7 meters in diameter) making them much more difficult to measure than the primaries. To achieve the highest possible image quality, the mirrors must be polished to the correct shape within 20 nm rms, so they need to be measured to an accuracy of 10 nm rms. It is difficult and expensive to achieve this measurement accuracy for the large secondaries using traditional methods. The classical Hindle test requires interferometry over long paths and a large, high-quality auxiliary mirror. A variation of this test replaces the large mirror with a partially transmitting lens that is only slightly larger than the test mirror. For large secondaries this shell is expensive because it must be made of extremely high quality glass and must be figured and supported accurately.

0277-786X/97/$10.00

Two new highly accurate and efficient measuring techniques were implemented at a new facility built at the Steward Observatory Mirror Lab (SOML) for fabricating and testing large secondary mirrors. The polished surfaces are measured interferometrically using full-aperture test plates with computer-generated holograms (CGH's).[1] This optical test is accurate to less than 10 nm rms and is performed with the secondary face down in the as-used orientation for zenith pointing. A swing-arm profilometer[2] is used to guide the aspherizing and loose-abrasive grinding. This instrument, which is mounted to the polishing machine, measures surface profiles with 50 nm rms accuracy. Both of these tests have been successfully used at the Steward Mirror Lab for measuring the 1.15-m secondary for the Sloan Digital Sky Survey Telescope[3] and are planned for secondary mirrors for U of A telescope projects listed in Table 1.

Table 1. Convex secondary mirrors to be measured using CGH test plates.

	MMT	ARC F/8	Sloan	MMT *f*/9	MMT *f*/15	MMT *f*/5	LBT *f*/4
Diameter (mm)	260	838	1143	996	620	1653	1170
Radius of curvature R (mm)	1484	3167	7194	2806	1663	5022	3294
Conic constant K	-1.430	-2.185	-12.110	-1.749	-1.397	-2.640	-3.236
Surface sagitta (mm)	5.7	27.7	22.7	44.2	28.9	68.0	51.9
P-V asphere (microns)	3.9	66.3	108.4	152.2	87.7	304.0	331.4
Focal ratio	2.85	1.89	3.15	1.41	1.34	1.52	1.41

2. INTERFEROMETRY USING CGH TEST PLATES

Convex spherical surfaces are commonly measured with matching concave test plates. When the test plate is supported near the convex optic and illuminated with sufficiently coherent light, fringes of interference show the shape difference between the two parts. The shape of the concave master sphere may be measured independently from its center of curvature. In a similar manner, convex *aspheric* surfaces may be tested using matching concave aspheric test plates. The obvious difficulty with this method is the requirement of making and measuring a concave master asphere for each convex optic.

The holographic test simplifies this by using a test plate with concave spherical surface, which is easy to manufacture and measure. The aspheric departure of the secondary is compensated by diffraction from a circular computer-generated hologram (CGH) or zone plate that is fabricated onto the concave spherical reference surface of the test. The test is performed by supporting the holographic test plate a few millimeters from the secondary mirror and illuminating with laser light (see Fig. 1). The interference pattern is viewed through the test plate and imaged onto a CCD camera for analysis. By pushing the test plate, phase shifting interferometry is used to obtain high resolution data.

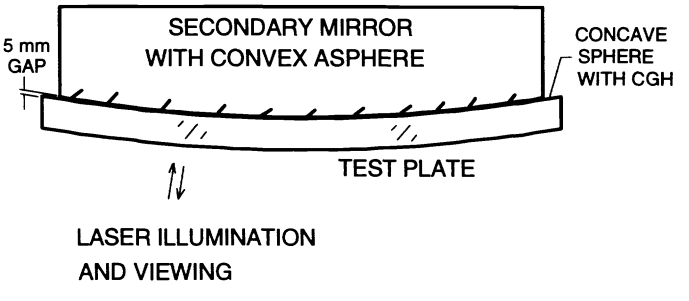

Figure 1. Layout of holographic test of a secondary mirror. The test plate has a reference spherical surface with a ring pattern drawn onto it.

This test is implemented for measuring the secondary mirrors at Steward Observatory face-down, as they are used at zenith in the telescope. This has the obvious advantage of measuring support errors. It also gives easy access for measuring the spherical reference surface that has the hologram. When the secondary is removed, the concave test plate is interferometrically measured from above and shape errors can be subtracted from the secondary measurement.

2.1 DEFINITION OF REFERENCE AND TEST WAVEFRONTS

The holographic test uses the interference between a reference and a test wavefront to determine the shape of the convex optic. Light diffracted from the hologram on the spherical surface forms the reference wavefront and light reflected from the secondary forms a test wavefront (see Fig. 2). The test plate is illuminated with light that is transmitted to strike the secondary mirror at normal incidence for all points on the mirror. This light reflects back onto itself to form the test wavefront. The reference wavefront is formed by diffraction from the ring pattern on the reference sphere. The CGH is designed to diffract this reference beam to match an ideal test wavefront, so this beam also retraces the incident path. (This is known as a Littrow configuration for a grating.)

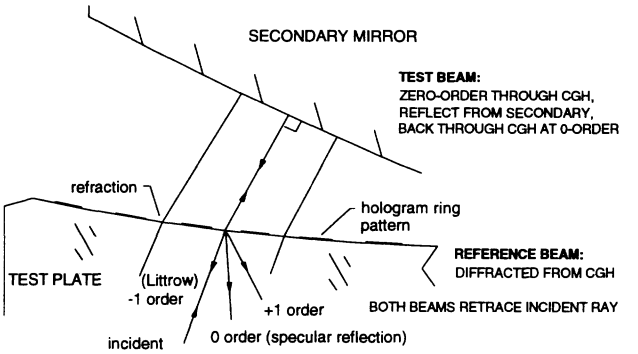

Figure 2. Definition of reference and test wavefronts. The reference beam diffracted from the hologram interferes with the test beam reflected from the secondary.

To perform a measurement, laser light from a point source is expanded. The reflected wavefronts converge to a conjugate image point, where an aperture blocks undesired orders of diffraction. It is important to note that the reference and test beams are coincident everywhere except in the air gap between the CGH and the secondary. So errors in the illumination optics, including refractive index variations in the test plate are common for both wavefronts and do not affect the measurement. This allows low-quality optics to be used for every part in the test except for the spherical reference surface.

2.2 OPTICAL DESIGN OF CGH TEST

The design of the holographic test is divided into the hologram design and the illumination optical system design. The hologram designs involve calculating the ring positions to give the desired phase of the reference wavefront and fixing the width of the rings to match the amplitudes of the test and reference beams. The illumination system is designed to bring the rays of light into the test at the correct angle, to separate diffraction orders, and to minimize the mapping distortion on the image.

The wavefront diffracted by the hologram must include power so that different orders of diffraction will come to focus at different axial positions. A stop at the correct position is used to isolate the desired diffracted order. Plots of the wavefront shape and the ring spacing are shown in Figs. 3 and 4 for the CGH test of the secondary mirror for the Sloan Digital Sky Survey Telescope. The different curves correspond to different amounts of power in the holograms. The amount of power is indicated by specifying the radial zone that has the same line spacing as that at the edge. This zone is indicated by the numbers shown to the right of the curves.

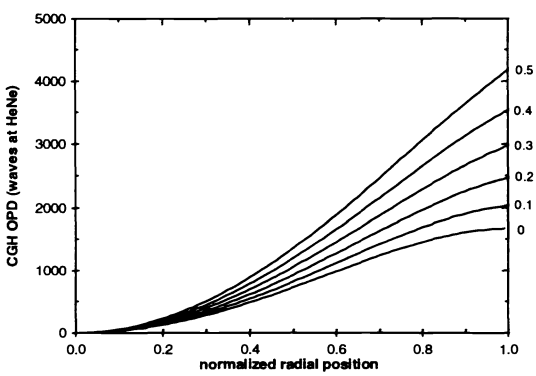

Figure 3. Variation of optical path function defined by hologram with radial position for different amounts of focus.

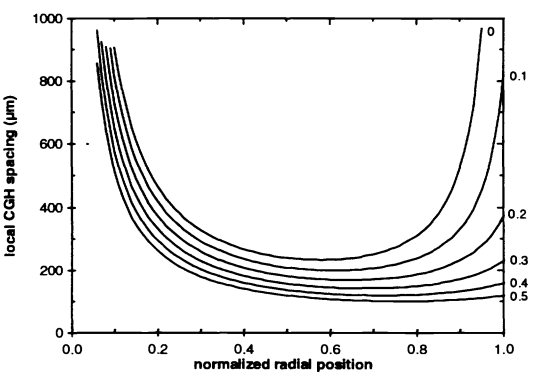

Figure 4. Center to center ring spacing as function of radial position for different amounts of focus.

The width of the rings is picked to match the intensities of the test and reference wavefronts, giving a high contrast interference pattern. Both reference and test beams are modulated by the hologram, and the far-field distribution is calculated by taking a Fourier transform. The phase of the reference and test wavefronts are shown to be independent of the line width. We have found that patterns with 18% duty cycle (ratio of line width to spacing) give perfect contrast for measuring bare glass surfaces. We have also demonstrated that we can use a single hologram with 35% duty cycle to measure both bare glass and aluminized surfaces with 70% contrast fringes.

The illumination system must force all the rays to hit the secondary at normal incidence and must allow a distortion-free image of the secondary at the camera plane. The techniques for designing these systems are given in detail elsewhere.[4,5] In order to isolate the desired orders of diffraction, the imaging system is limited to collecting light with up to ±1 mrad slope error at the secondary. Errors larger than this will cause loss of data. It is important to provide a distortion-free image of the secondary to minimize coupling between alignment errors and surface measurement errors. The illumination system implemented at SOML (See Fig. 5.) uses two mirrors that resemble a Cassegrain telescope. We have also built systems to measure smaller aspheres, up to 400 mm, that use low-quality acrylic lenses to provide the illumination.

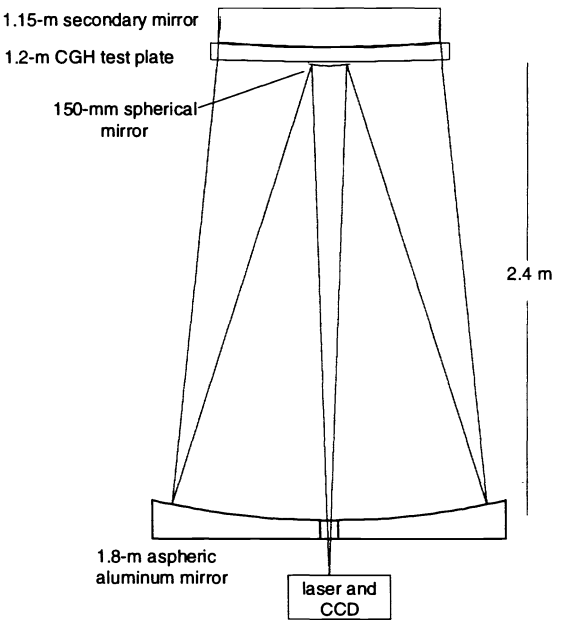

Figure 5. Layout for the CGH test of the Sloan Secondary.

The alignment requirements for the illumination system must only meet the 2 mrad blur circle requirement. The alignment of the secondary to the test plate is guided by the interference pattern. The mirror is tilted, translated axially and translated laterally to eliminate tilt, focus, and coma from the interference pattern. Once the optic is aligned, the secondary radius of curvature R is measured by measuring the gap between the optics. The centration of the asphere on the blank is determined by measuring the lateral position of secondary relative to the test plate. There is a coupling between errors in R and errors in the conic constant K given by[5]

$$\frac{\Delta K}{K} = -\frac{\Delta R}{R}. \tag{1}$$

3. IMPLEMENTATION OF CGH TEST FOR LARGE SECONDARIES

The CGH test is implemented in the SOML shop using a newly constructed dedicated secondary test system (STS). This system uses a small test tower attached to our larger 24-m vibration isolated tower. The equipment, shown in Fig. 6, was built for measuring secondary mirrors up to 1.8 meters in diameter. The test tower has three levels: a platform with an interferometer that measures the test plates, a platform that supports the test plates and secondary mirrors, and a lower platform that holds the illumination primary and the projection and imaging optical system.

The CGH test is illuminated in a scheme that resembles a Cassegrain telescope with a 1.8-m solid aluminum primary. A laser source is projected through a center hole in the aluminum reflector to a 15 cm secondary reflector. Light reflected from the secondary fills the illumination primary, which reflects the light to illuminate the holographic test. The light from the test retraces its path to go through the center hole in the primary. This light is imaged onto a CCD camera to show the fringes of interference. It is important that both the reference and test wavefronts are coincident through this system, so the optics do not have to be made to high quality. Our system causes errors in slope as large as ±1 mrad without affecting the test. We also have some severe striae in the test plate that cause larger slope errors which cause the light to miss the imaging system altogether, leaving small gaps in the data.

The secondary mirrors are supported with the optical surface down, in the orientation they will be used for zenith pointing in the telescope. The mirrors are transported from the polishing machine to the STS and then flipped using a special mechanism and an overhead crane. The mirror cells are built to handle the polishing forces with the optic face up and to emulate the telescope support forces with the mirror surface facing down. The inverted cell is supported at three points on a frame in the STS. This frame is mounted on an azimuth bearing to allow full rotation of the optic relative to the test, which allows us to isolate azimuthal errors in the mirror from those in the test. The bearing is mounted on a six-axis positioning system that provides the fine movement needed to null the interference fringes. In practice, the mirror is moved in 5 axes to remove tilt, focus and coma from the interferogram. (The sixth degree of freedom gives a fine rotation about the optical axis.) The alignment system uses three pairs of stages, each pair consisting of two stacked linear stages with a small wedge between them. To get pure horizontal translation from the pair, the stages are run simultaneously in the same direction and they give pure vertical motion when they are driven in opposite directions. All six stages are synchronized under computer control to give the user independent control of x and y tilt, x and y coma, focus, and axial rotation. This system allows fine motion in all degrees of freedom for loads as large as 1000 kg. It also provides rigid support required by the interferometric tests.

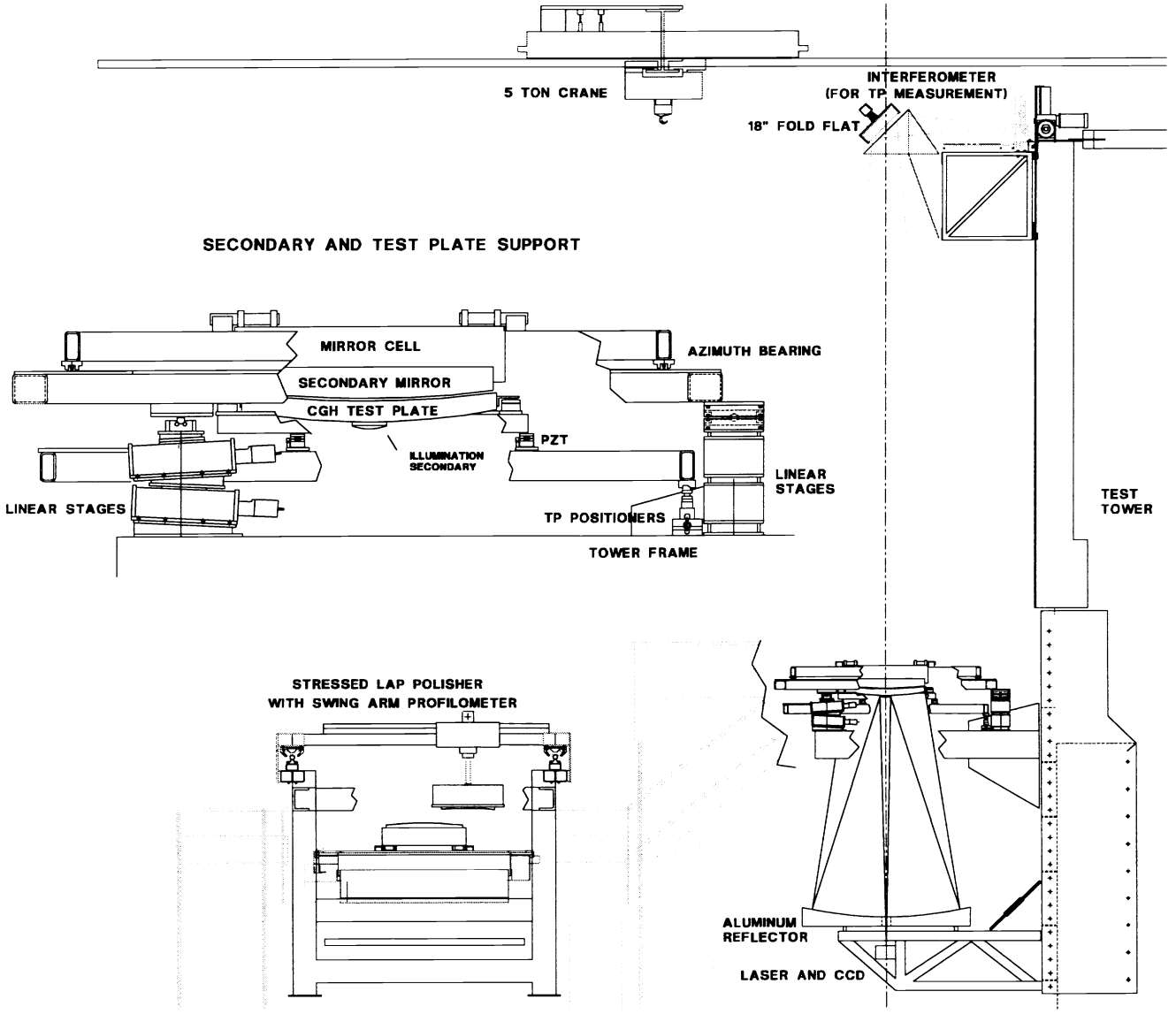

Figure 6. Layout of the secondary test system including details of optics support.

The illumination primary was turned from a solid piece of 6061 aluminum by an outside vendor. We subsequently ground and polished the bare aluminum to the correct aspheric shape with an acceptable finish. It is kinematically mounted on three jack screws that allow for its alignment. The convex secondary reflector has a spherical shape and is simply bonded to the test plate.

We currently have two completed holograms, the reference for the Sloan secondary and an 89-cm test hologram described below. The test plates were cast and slumped from E6 glass at Hextek and were polished by Rayleigh Optical. They are held in the STS by a distributed set of hydraulic actuators pushing on support brackets bonded the edges of the glass. The actuators are mounted to in a steel ring that is supported at three points on mechanisms with piezo transducers (PZT's). High resolution surface measurements are made using phase shifting interferometry by pushing the test plates, while video images of the fringe patterns are captured and processed in a PC.

The surface figures of the test plates are measured *in situ* using a phase shifting Shack cube interferometer supported in the tower above the optic. The test is aligned remotely by steering a 10 cm fold flat and by translating the interferometer on a linear stage. The overhead crane must go over the optical axis, so the optics for the test plate measurement were built with the ability to move out of the way. We achieve this by using a 46 cm fold flat that is swung to the side to clear the crane. This entire system is attached to a platform that can be driven to the proper height for each test plate. The radius of curvature of the test plate is measured to ±0.5 mm using a calibrated steel tape.

4. FABRICATION OF HOLOGRAMS

Equipment and techniques were developed at the University of Arizona for fabricating the large computer-generated holograms onto curved surfaces. A large laser writing machine was built to write binary zone plates onto spherical surfaces up to 1.8 meters in diameter and with focal ratios as fast as $f/1$. This machine writes 6 μm to 150 μm wide zones with radial position accuracy better than 1 μm rms over the full diameter. The problems of applying and processing photoresist are avoided by defining the patterns using a simple thermochemical technique. Several holograms up to 1.2 meters across have been successfully written and tested.

Circular patterns are optimally fabricated using polar coordinate machines that expose rings by rotating the substrate under a fixed writing beam. The hologram accuracy depends on the quality of the rotation bearing, the ability to control the radial position of the writing beam, and the ability to locate the center of rotation. This geometry has been used by several groups for writing accurate zone plates onto small, flat substrates.[6,7,8] Also, diffractive optics for infrared applications have been turned on lathes with single-point diamond tools.

The writer uses cylindrical r, θ, and z coordinates, where a write-head that controls and focuses the laser beam is moved in the r and z directions with horizontal and vertical linear stages. The substrate is rotated face up using a precise vertical axis air spindle. The laser itself is mounted rigidly to the frame and the collimated beam is directed to the optics head using mirrors and prisms. The beam is shaped, measured, modulated and brought to focus at $f/6$ onto the hologram substrate.

The accuracy of the radial position is achieved using laser interferometers, active control for laser beam drift, a rigid athermal support frame, and a temperature controlled enclosure. Two interferometers are used to measure the radial position and tilt of the write head. The interferometers are mounted to the frame so that the distance from the reference mirror to the axis of rotation does not change with temperature. The reference mirror on the write head is also mounted athermally so the distance from this mirror to the writing beam is not temperature dependent.

The write-head is a 16 x 16 x 32 cm box full of optics and electronics for beam measurement and control. The writing power and fine steering of the beam are controlled using an acousto-optic modulator (AOM). This device converts an RF signal into acoustic waves in a crystal. The crystal is then aligned so the acoustic waves act as a Bragg diffraction grating. The amplitude of the RF driving signal is varied to adjust the diffraction efficiency, thus the power of the writing beam. The frequency of the RF signal is varied to change the diffracted angle, which translates the focused spot over a ±80 μm region. The AOM and drive electronics allow 300 kHz bandwidth for both the power and position control, although we run them much slower.

Rings with different widths are written by rapidly scanning the 6 μm spot radially with the AOM. The 80 MHz RF signal is frequency modulated with a 5 to 70 kHz sawtooth waveform with amplitude proportional to the desired line width. This causes the beam to sweep back and forth radially to fill in the complete line. The scanning signal is AC coupled to ensure that it affects only the width of the scan, and does not shift the center. The AC signal is summed with a DC voltage from a DAC that shifts the line, but does not change its width. The light passes through the AOM and a filter (to isolate the correct order of diffraction), and then a beamsplitter which taps off 3% of the power for measurement. The remaining 97% is focused onto the substrate. Half of the measurement light is sent to a photodiode for measuring the writing power. The writing power is stabilized with an analog servo that uses feedback from the photodiode and amplitude control with the AOM. The rest of the split-off light is projected onto a CCD array to form a magnified image of the writing spot. Since the scan frequency is many times faster than the video rate, the image is blurred out to appear as a continuous line. The CCD image is digitized and processed in real time to measure the center position and the width of the scan. This information is coupled with the position data from the interferometers and fed back to the AOM control to adjust the center position and width of the scan.

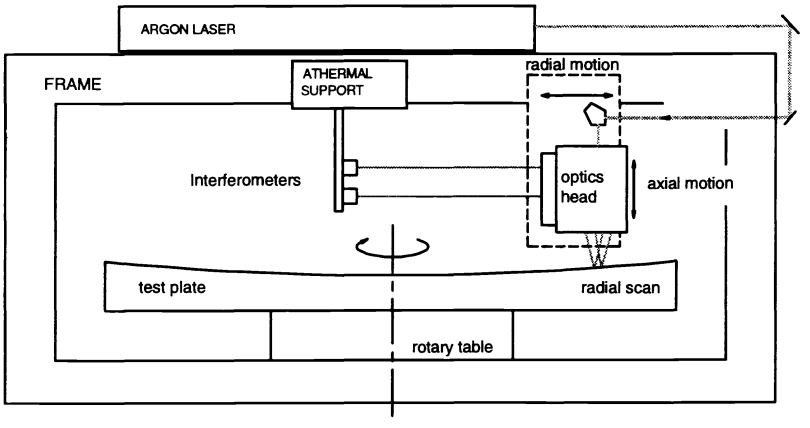

Figure 7. Schematic drawings of writing machine.

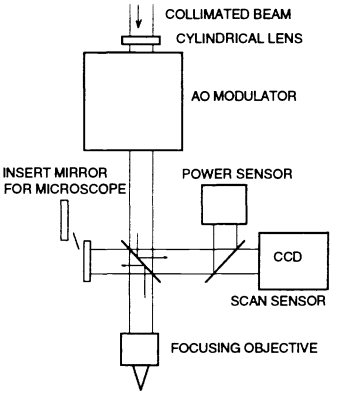

Figure 8. Optics head schematic

The writer has a microscope mode that uses a fold mirror to focus light reflected from the substrate onto the CCD camera. This gives an image of the surface with sub-micron resolution. This image is used primarily for setting focus and finding center. The focus is set with 5 μm resolution by using the microscope to visually inspect the image of the writing spot. Since the depth of focus is large, we do not require an auto-focus system. We find the best focus for two points on the mirror and follow the trajectory defined by these points and the known shape of the substrate. The center of rotation is found to 1 μm by burning a small ring, 20 - 60 μm in diameter and aligning it with the writing beam using the microscope.

The procedure for writing the holograms is to first align and calibrate the machine so that the metrology is accurate, the servos are properly tuned and the beam shape is acceptable. Then the substrate is mounted, centered and leveled. The center of rotation and the two points where the beam is focused onto the substrate are defined. A small test pattern is written outside the clear aperture to help define the target writing power. The hologram is written, generally starting on the outside. When the writing is finished, we verify the center of rotation to measure any shifts that may have occurred during writing.

Computer-generated holograms are commonly manufactured by exposing thin layers of photoresist with near-UV light. The lithography technology is mature for small, flat parts, however it is difficult to apply and develop resist on large, curved substrates. These difficulties are avoided by using a different fabrication method -- thermochemical writing. This technique avoids the use of photoresist by writing the image directly onto a chrome film with a laser beam using a thermochemical effect. The laser exposes the chrome by heating it, which causes an oxidation layer at the surface. After writing the complete pattern and creating this oxide latent image, the optic is immersed into a caustic bath that dissolves the bare chrome preferentially to the chrome oxide. So after developing, a pattern of chrome remains where the laser had exposed the surface and created the oxide layer.

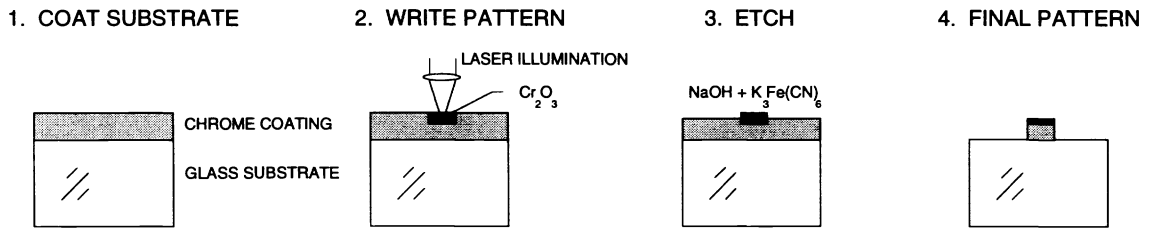

Figure 9. Pattern generation using laser induced oxidation.

We use a solution of NaOH and $K_3Fe(CN)_6$ to preferentially dissolve the un-oxidized metal. Tests have shown that the chemical concentration and temperature do not affect this selectivity, but only change the etch rate. A large test plate is developed by putting a stopper in the center hole and filling the volume created by the concave surface with dilute etchant. After 20 to 30 minutes when the pattern is fully etched, the stopper is pulled and the fluid drains out the center hole. Once it is rinsed and dried, the hologram is ready for use in an optical test.

Fabrication and measurement of an 84-cm pattern

A large CGH was fabricated and used to certify the accuracy of the writer. The hologram was designed to be fabricated onto a spherical surface so that the light diffracted into the second order will appear as a perfect spherical wavefront with radius of curvature slightly longer than the substrate radius. The hologram accuracy was measured using an interferometer with a HeNe source. First the substrate figure was measured (0-order for the hologram), and then the interferometer was translated 133 mm to measure the second order light, as shown in Fig. 10. The difference between the two measurements was used to determine the error due to the hologram. The second order of diffraction was used rather than the first to make the test double-sensitive to hologram errors.

The hologram with 1694 rings was written in 5 hours on the large hologram writer. The centering test at the completion of writing demonstrated that the machine was stable to < 1 μm. The hologram was etched and mounted in the vibration-isolated tower at the Steward Mirror Lab. The measurements at zero and second orders show the surface figure to be around 0.08 waves rms with difference of only 0.008 λ rms (See Fig. 11). Writer errors would cause mostly axisymmetric errors, which were only 0.0016 λ rms. This confirms the writer accuracy of < 0.7 μm rms for radial positioning.

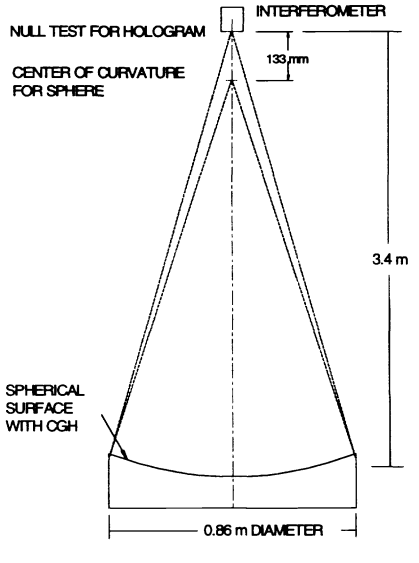

Figure 10. Layout for testing hologram by measuring 0 and 2nd order.

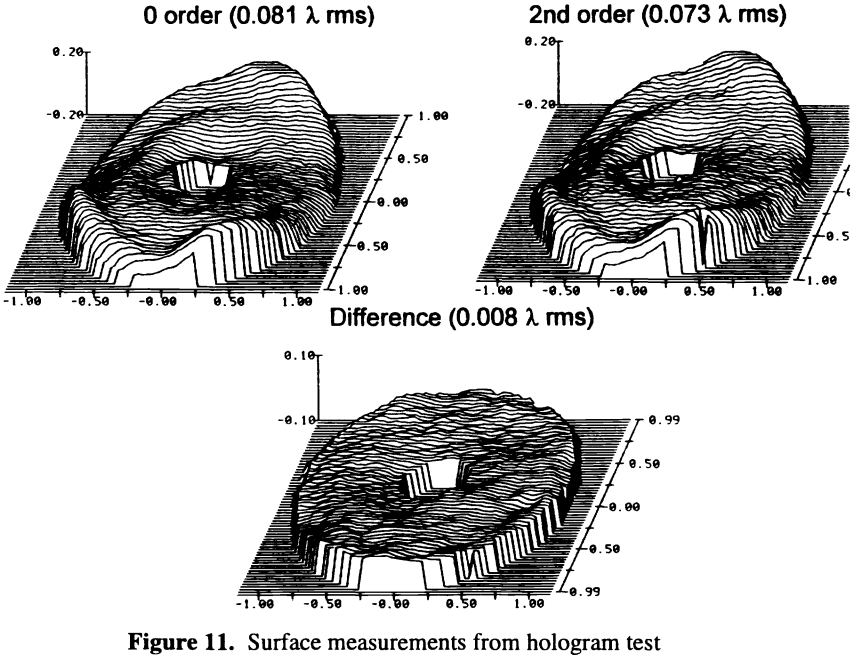

Figure 11. Surface measurements from hologram test

5. SECONDARY MEASUREMENTS USING CGH TEST PLATES

We have measured several secondary mirrors using CGH test plates. A CGH test of one of the existing secondary mirrors for the MMT telescope shows agreement to a few nanometers with a Hindle test of the same mirror.[9] The CGH test using Steward-written holograms has also been implemented by two other optical shops. The 1.15-m secondary mirror for the Sloan Digital Sky Survey Telescope was polished in our shop and measured with a CGH test plate. The measurements were made using the secondary test system (STS) described above with the mirror surface face-down. The CGH test was demonstrated to be quite efficient; the mirror could be removed from the polishing machine, measured, and return to the polisher in about two hours. Random measurement errors of 5 nm due mostly to vibration were quickly averaged in several measurements. The figure of the test plate reference surface was routinely measured *in situ* using the Shack cube interferometer fixed above the optic. Spherical aberration of 185 nm rms in the test plate surface was compensated by the hologram. The remaining 82 nm figure errors were directly removed from the secondary measurement. Analysis of this CGH test shows overall accuracy of 4.1 nm rms with 3.2 nm from the test plate figure, 1.5 nm from the hologram, and 1.8 nm from various second order effects.. It is interesting that the dominant source of error in the test of this steep asphere is a concave face-up spherical surface.

The test plate for the Sloan measurement was cast from blocks of E6 glass, which led to severe refractive index inhomogeneities. The striae in the glass, which shows up even upon visual inspection, causes strange-looking intensity variations in the interferogram, shown in Fig. 12. However, the surface measurement from the phase shifting interferometry, shown in Fig. 13, shows no correlation between the calculated phase and the striae. Also a rotation test did not show any fixed measurement errors other then the expected contribution from surface figure.

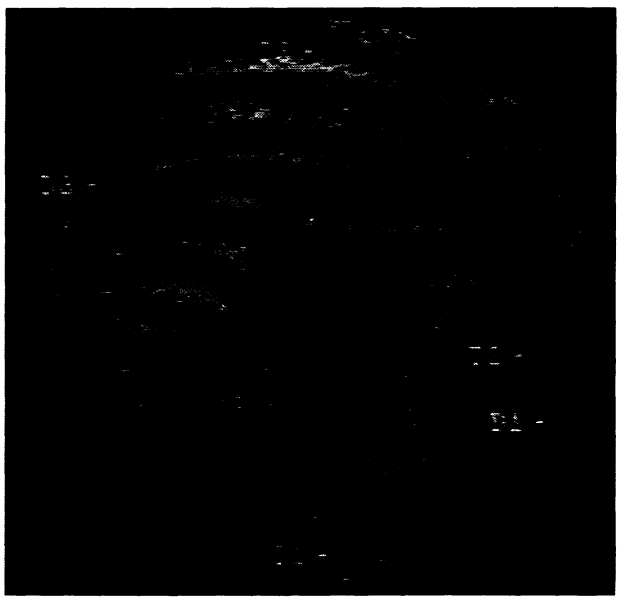

Figure 12. Interferogram from the CGH test of the Sloan secondary mirror. The pattern shows excellent contrast overall, but lower intensity in regions of sharp striae. These irregularities do not show up in the surface measurement.

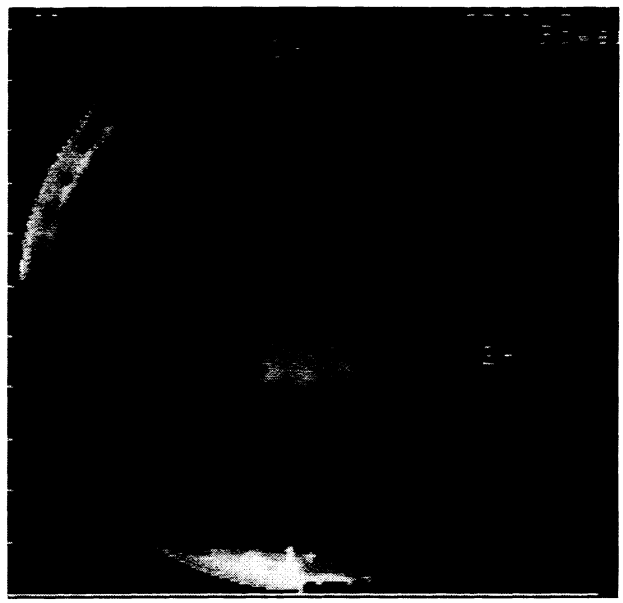

Figure 13. A gray-scale plot showing a measurement created by phase shifting the interferogram in Fig.12. This shows 82 nm rms, 400 nm P-V surface errors due to both the secondary and the test plate, but no effect of the striae in the glass.

The CGH test of this mirror shows the figure to be 46 nm rms at the time of writing this paper. A map of this surface, shown in Fig. 14, has spatial resolution of about 200 pixels across the 1.15-m diameter. The structure function of this surface shows that it exceeds the 0.2 arc second FWHM specification by a factor of 5 at large scales and a factor of 2 at 2 cm scales on the mirror. We are continuing to improve the surface with a combination of small- and large- tool polishing.

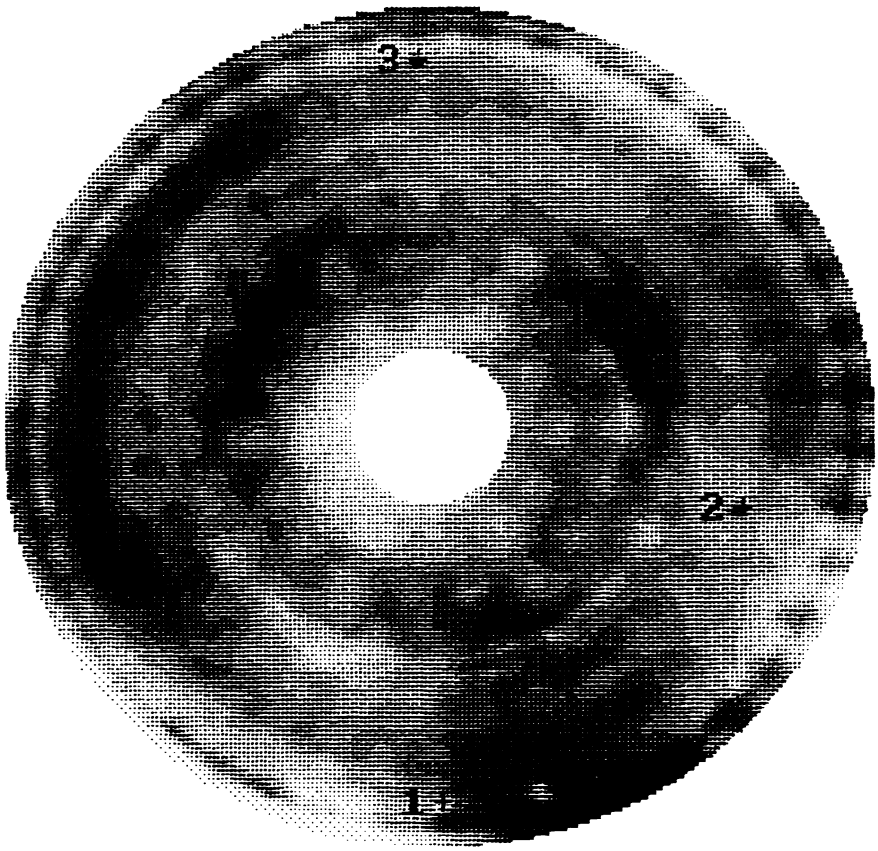

Figure 14. Surface measurement of Sloan secondary as of June, 1996. The gray scale plot shows the 46 rms surface with 20 nm rms contours over a full range of 300 nm.

6. SWING ARM PROFILOMETER

The rough-ground surfaces are measured using a swing-arm profilometer modeled after a machine built by Dave Anderson.[10] The profilometer is mounted to the secondary polishing machine to allow rapid measurements for guiding asphericizing and rough figuring. Our instrument measures surface profiles with 50 nm rms accuracy so it also provides verification of the interferometric CGH test.

The swing-arm profilometer uses an LVDT indicator at the end of an arm to make mechanical measurements of the optical surface. The geometry for this test is shown in Figure 15. The probe is mounted at the end of an arm that swings across the test optic such that the axis of rotation goes through the (virtual) center of curvature of the optic. The arc defined by the probe tip trajectory (for no change in probe reading) lies exactly on a spherical surface defined by this center. This is the geometry used for generating spherical surfaces using cup wheels. For measuring the aspheric optics, the probe, which is aligned so its travel is in the direction normal to the optical surface, reads only the surface departure from spherical.

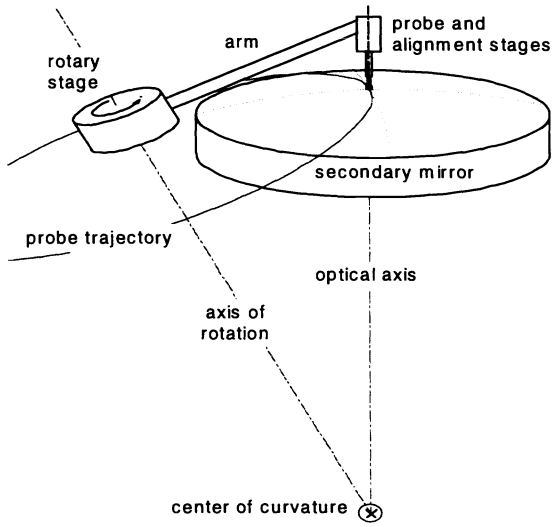

Figure 15. Geometry for the swing arm profilometer.

This simple instrument achieves its high accuracy by using the advantageous geometry, a high quality rotary stage and LVDT, and computer control. The indicator is always held normal to the optical surface and its total travel is only as much as the aspheric departure of the mirror. Thus the positioning requirement for the probe is relaxed by orders of magnitude relative to that for an x, z machine. The rotary air bearing with integral motor and encoder was demonstrated to run true using capacitance gauges. The air bearing LVDT probe was calibrated to 0.1 μm P-V over its full 1000 μm travel. The machine is controlled and the data is processed efficiently on a PC computer.

Misalignment of the axis of rotation will cause measurement errors that appear as tilt and focus in the data.[2] These terms are used to align the profilometer the same way tilt and focus fringes are used to align an interferometric test. The instrument is mounted on a two-axis rotary table to allow these adjustments.. The mount for the probe at the end of the arm allows 5-axis adjustment to align the probe with the arm and the optic. The flexure of the arm and probe mount due to gravity does not significantly affect the surface measurement because it causes only a quadratic change in the measurement, which corresponds to power or focus in the data. This was analyzed for the measurement of a 1.2-m mirror with 300 μm asphericity and shown to cause less than 10 nm error in the surface measurement for an arm with 10 Hz resonance.[2] Since power is removed from the data the radius of curvature of the secondary must be determined by another method; we use a sub-aperture test plate during grinding and the CGH test for the polished surface.

The SOML profilometer is mounted rigidly to the stressed-lap polishing machine to allow efficient measurements while the mirror is on the turntable. (See Fig. 16.) The arm itself is balanced so it does not exert any changing forces on the frame while it scans. The machine is supported on three air bags to isolate it from vibration and varying loads from the floor. The combination of electrical noise, random variations in the probe-glass interface, and mechanical instabilities gives measurement errors around 100 nm rms over the 10 minutes required for a full scan. After these random errors are averaged out, the fixed error in the bearing of around 0.040 μm rms remains.

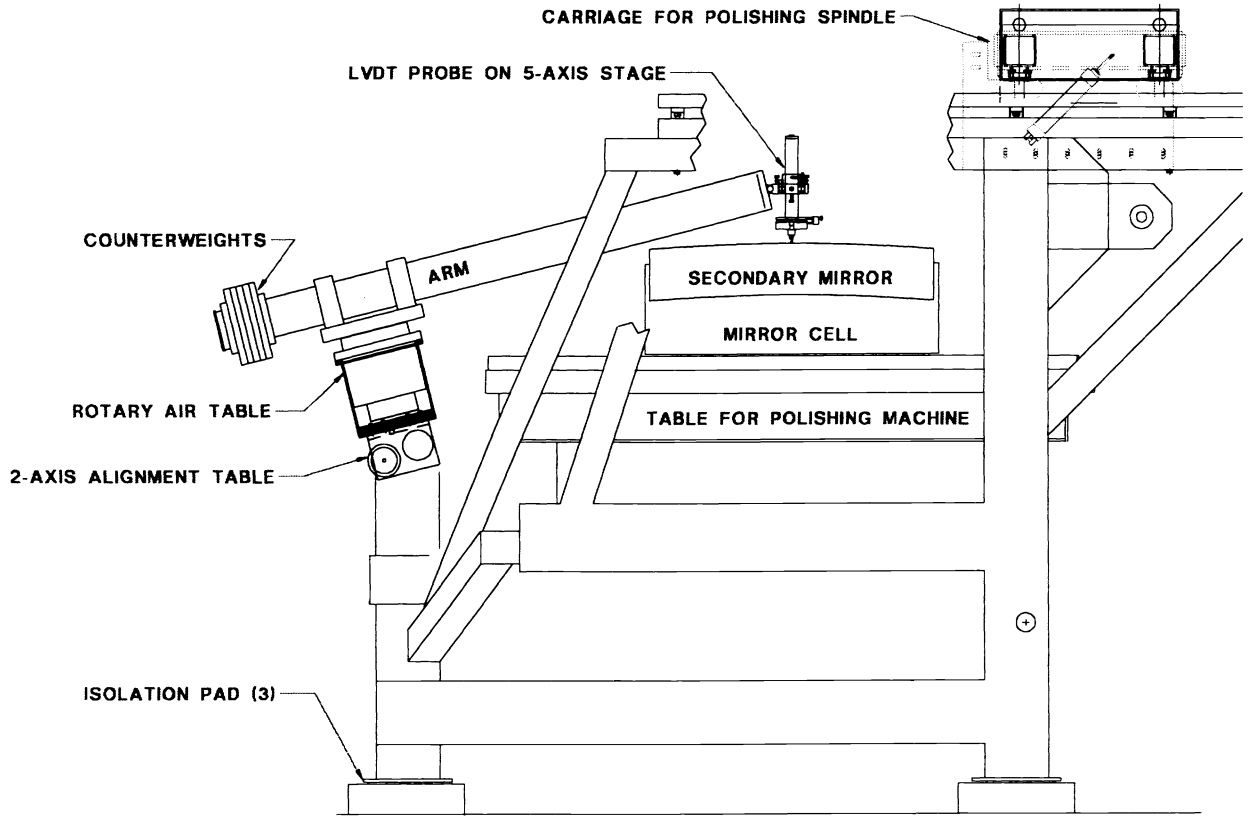

Figure 16. Layout of swing arm profilometer mounted to our 1.8-m stressed-lap polishing machine.

The accuracy of the profilometer was assessed using two methods. When the Sloan mirror was nearly spherical, the same arc on the surface was scanned with the arm mounted at different orientations on the rotation stage. The difference between these scans shows the expected bearing errors of 40 nm rms. Also the profilometry of the nearly finished mirror shows excellent agreement with the data from the holographic test plate, as shown in Fig. 17. A direct comparison is difficult when the mirror has significant non-axisymmetric errors because the profilometer data follows an arc on the surface and the plots from the interferometry show profiles across lines. However, since both have nearly the same magnitude of 82 to 86 nm rms, the agreement must be much less than this amount. We expect better results when we reproduce this test on the finished mirror.

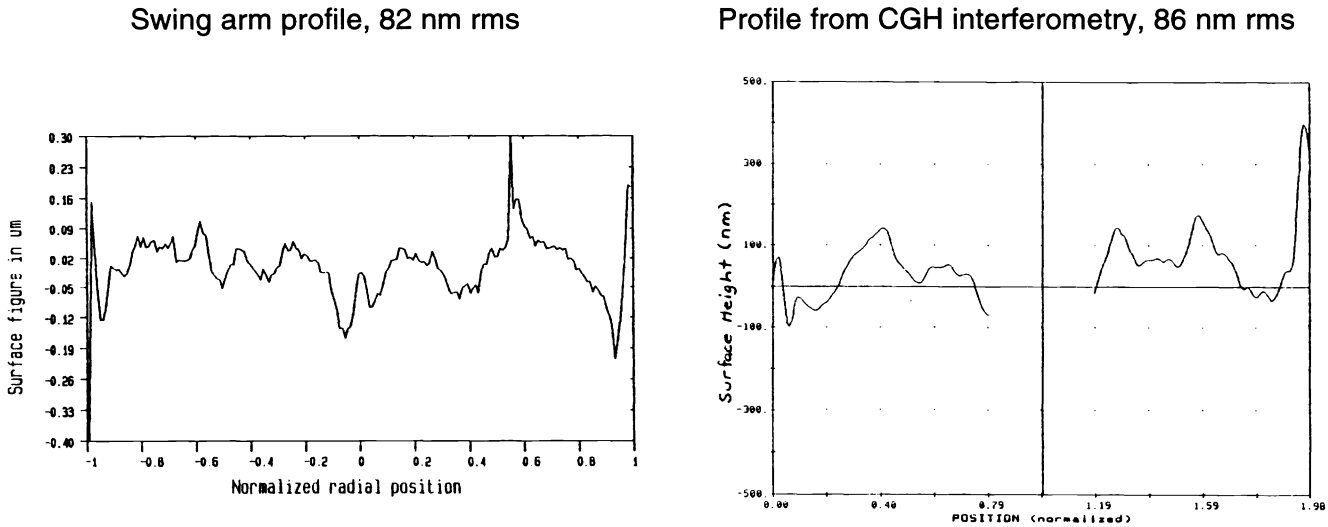

Figure 17. Comparison between a swing arm measurement and a diametrical profile from CGH interferometry.

7. CONCLUSIONS

The Steward Observatory Mirror Lab has invested in new equipment and techniques for accurately measuring large steep secondary mirrors. We will use the swing arm profilometer and interferometry with holographic test plates to guide the fabrication of secondary mirrors for University of Arizona telescopes. We also hope to share our technology for other applications.

8. ACKNOWLEDGMENTS

Much of the equipment reported in this paper was designed and built by the capable technical staff at Steward Observatory. This work was funded in part by the Sloan Foundation through the Astrophysical Research Consortium.

REFERENCES

1. J. H. Burge and D. S. Anderson, "Full-aperture interferometric test of convex secondary mirrors using holographic test plates," Proc. SPIE **2199**, (1994).
2. D. S. Anderson and J. H. Burge, "Swing-arm profilometry of aspherics," Proc. SPIE **2536**, (1995).
3. B. K. Smith, J. H. Burge, and H. M. Martin, "Fabrication of the 1.2 m secondary mirror for the Sloan Digital Sky Survey," OF&T Tech. Dig. **7**, (1996).
4. J. H. Burge, "Applications of computer-generated holograms for interferometric measurement of large aspheric optics," Proc. SPIE **2576**, (1995).
5. J. H. Burge, "Fizeau interferometry for large convex surfaces," Proc. SPIE **2536,** (1995).
6. V. P. Koronkevich, *et al*, "Fabrication of kinoform optical elements," Optik **67**, (1984).
7. W. Goltsos and S. Liu, "Polar coordinate laser writer for binary optics fabrication," Proc. SPIE **1211**, (1990).
8. T. Nomura, *et al.*, "An instrument for manufacturing zone-plates by using a lathe," Prec Eng **16**, (1994).
9. J. H. Burge, *et al.*, "Measurement of a convex secondary mirror using a holographic test plate," Proc. SPIE **2199,** (1994).
10. D. S. Anderson, R. E. Parks, T. Shao, "A versatile profilometer for the measurement of aspherics," OF&T Workshop Tech. Dig, (1990).